

Hot Plasma and Energetic Particles in Neptune's Magnetosphere

S. M. KRIMIGIS, T. P. ARMSTRONG, W. I. AXFORD, C. O. BOSTROM, A. F. CHENG, G. GLOECKLER, D. C. HAMILTON, E. P. KEATH, L. J. LANZEROTTI, B. H. MAUK, J. A. VAN ALLEN

The low-energy charged particle (LECP) instrument on Voyager 2 measured within the magnetosphere of Neptune energetic electrons (22 kiloelectron volts $\leq E \leq 20$ megaelectron volts) and ions (28 keV $\leq E \leq 150$ MeV) in several energy channels, including compositional information at higher (≥ 0.5 MeV per nucleon) energies, using an array of solid-state detectors in various configurations. The results obtained so far may be summarized as follows: (i) A variety of intensity, spectral, and anisotropy features suggest that the satellite Triton is important in controlling the outer regions of the Neptunian magnetosphere. These features include the absence of higher energy (≥ 150 keV) ions or electrons outside $14.4 R_N$ (where R_N = radius of Neptune), a relative peak in the spectral index of low-energy electrons at Triton's radial distance, and a change of the proton spectrum from a power law with $\gamma \geq 3.8$ outside, to a hot Maxwellian ($kT \approx 55$ keV) inside the satellite's orbit. (ii) Intensities decrease sharply at all energies near the time of closest approach, the decreases being most extended in time at the highest energies, reminiscent of a spacecraft's traversal of Earth's polar regions at low altitudes; simultaneously, several spikes of spectrally soft electrons and protons were seen (power input $\approx 5 \times 10^{-4}$ ergs $\text{cm}^{-2} \text{s}^{-1}$) suggestive of auroral processes at Neptune. (iii) Composition measurements revealed the presence of H, H₂, and He⁴, with relative abundances of 1300:1:0.1, suggesting a Neptunian ionospheric source for the trapped particle population. (iv) Plasma pressures at $E \geq 28$ keV are maximum at the magnetic equator with $\beta \approx 0.2$, suggestive of a relatively empty magnetosphere, similar to that of Uranus. (v) A potential signature of satellite 1989N1 was seen, both inbound and outbound; other possible signatures of the moons and rings are evident in the data but cannot be positively identified in the absence of an accurate magnetic-field model close to the planet. Other results include the absence of upstream ion increases or energetic neutrals [particle intensity (j) $< 2.8 \times 10^{-3} \text{ cm}^{-2} \text{ s}^{-1} \text{ keV}^{-1}$ near 35 keV, at $\sim 40 R_N$] implying an upper limit to the volume-averaged atomic H density at $R \leq 6 R_N$ of $\leq 20 \text{ cm}^{-3}$; and an estimate of the rate of darkening of methane ice at the location of 1989N1 ranging from $\sim 10^5$ years (1-micrometer depth) to $\sim 2 \times 10^6$ years (10-micrometers depth). Finally, the electron fluxes at the orbit of Triton represent a power input of $\sim 10^9$ W into its atmosphere, apparently accounting for the observed ultraviolet auroral emission; by contrast, the precipitating electron (> 22 keV) input on Neptune is $\sim 3 \times 10^7$ W, surprisingly small when compared to energy input into the atmosphere of Jupiter, Saturn, and Uranus.

THE PRIMARY SCIENTIFIC OBJECTIVES of the LECP investigation during the encounter of Voyager 2 with Neptune were to discover the nature of the planet's magnetosphere (if any), to measure the intensity, energy spectra, composition, angular distributions, and spatial and temporal characteristics of magnetospheric ions ($E \geq 28$ keV) and electrons ($E \geq 22$ keV), and to determine the nature and importance of the interactions of these particle populations with Triton and with the subsequently discovered Neptunian satellites N1-N6, as

well as the planetary rings. The LECP instrument has two sensor systems: the low-energy particle telescope (LEPT) and the low-energy magnetospheric particle analyzer (LEMPA), both of which have a large number of solid-state detectors that can be used in various coincidence-anticoincidence configurations. In order to obtain angular distributions, the detector heads are mounted on a platform that rotates through 360° on the three axis-oriented Voyager spacecraft. One of the angular positions places the sensors behind a 2-mm-thick aluminum

shield to obtain an accurate measure of background. Because of several spacecraft constraints during the Neptune encounter, the detector heads were kept stationary either in sector 1 or sector 7, with the exception of periodic (every 6 min) 360° scans of 48 s or 96 s in duration. These periodic scans were interrupted during inbound and outbound crossings of the planetary equatorial plane so that the instrument's sensitive detectors would be protected from the impact of micron-sized particles co-orbiting with the planet. Continuous, 360° scans of the instrument, one scan per 6.4 min, were used 12 hours before the closest approach and resumed ~ 24 hours after periapsis. A full description of the LECP instrument is contained elsewhere (1).

Overview. The Voyager discovery of the magnetosphere of Neptune, as recorded by the LECP instrument, is summarized in Fig. 1, which shows a color spectrogram as a function of spacecraft event time (SCET) of the intensities of ions and electrons for a 2-day period beginning on 24 August (day 236) at 1400 SCET. Before the inbound bow shock (BS) crossing, there was no hint of upstream ion activity, the first planet encountered by Voyager where this was the case (2). The absence at Neptune of clear, BS-associated proton and electron enhancements is also an unusual aspect of planetary magnetosphere encounters by Voyager. Further, there was only a modest increase in the proton intensities at the magnetopause (MP) and a marginal electron intensity increase, both of which are unique in the context of planetary magnetospheres investigated by Voyager. Only low-energy (≤ 150 keV) protons and electrons were present outside the radial location of Triton, and there were rapid increases in the intensities of higher energy particles inside that satellite's orbit (Fig. 1). A clear dip in the intensity of low-energy protons near the radial location of Triton is evident, both inbound and outbound. The peak intensity of the lowest energy electrons occurs at ~ 2330 SCET on 24 August, substantially earlier than the intensity peak for either the high-energy electrons (~ 0100 SCET) or the protons at any energy. Additional peaks in the lowest energy electron intensities oc-

S. M. Krimigis, C. O. Bostrom, A. F. Cheng, E. P. Keath, B. H. Mauk, Applied Physics Laboratory, The Johns Hopkins University, Laurel, MD 20707-6099.
T. P. Armstrong, the University of Kansas, Lawrence, KS 66044.

W. I. Axford, Max-Planck-Institut für Aeronomie, Postfach 60, 3411 Lindau, Federal Republic of Germany.
G. Gloeckler and D. C. Hamilton, University of Maryland, College Park, MD 20742.

L. J. Lanzerotti, AT&T Bell Laboratories, Murray Hill, NJ 07974.

J. A. Van Allen, University of Iowa, Iowa City, IA 52242.

curred at ~ 0315 SCET and again at ~ 0815 SCET, without corresponding intensity peaks occurring in the ions or high-energy electrons.

A most prominent feature in the spectrogram, particularly striking in the case of protons, is the virtual dropout in the intensities near closest approach at ~ 0400 SCET. In addition to the decrease in particle intensities around closest approach, the anticipated particle onset after magnetopause crossing did not occur until ~ 2000 SCET, and there was a relative decrease at ~ 1215 SCET on 24 August, mostly evident in the electron-intensity profile. This modulation of the intensities at about half the planetary rotation period of 16.1 hours suggests that the spacecraft may well have entered the magnetosphere at fairly high magnetic latitudes, with the decreases occurring at encounters of the planet's magnetic polar cap. This would also be consistent with the relative absence of magnetosheath-particle activity. The absence of significant energetic particle intensities after ~ 1600 SCET on 25 August suggests that the spacecraft may have entered the southern lobe of the mag-

netotail before exit from the magnetosphere (outbound MP) at ~ 0800 SCET on 26 August (day 238).

Fig. 2B shows a line plot of four selected energy channels from the data presented in Fig. 1 and a spectral index (assuming a power law) of electrons in the range $22 \leq E \leq 61$ keV (Fig. 2A). [A portion of the low-energy proton profile has been deleted because of possible contamination from high-energy (≥ 450 keV) electrons]. The general features discussed in connection with Fig. 1 are quite apparent in this plot as well. The orbit of Triton appears to be a controlling factor in determining the intensity onset of the more energetic ions and electrons, all of which are only significantly above background levels inside Triton's orbit. The spectral index shows a relative peak around Triton's distance, both inbound and outbound, with the electron spectrum becoming harder closer to the planet, until ~ 2400 SCET on 24 August.

The change in viewing directions of the LECP instrument between angular sectors 1 and 7 (which are 90° apart) provides a measure of the degree of anisotropy in the

particle distributions. Particle anisotropies became evident after ~ 0100 SCET on 25 August (diminished after ~ 0800 SCET) from the two levels of intensity seen in each profile. The radial variation of both electron and ion anisotropy amplitudes is consistent, with both species showing more sharply peaked angular distributions closer to Neptune. These preliminary analyses suggest that the anisotropy of lower energy particles increases more slowly than that of higher energy particles. Such behavior of anisotropies is consistent with magnetically trapped radiation at Earth, Jupiter, Saturn, and Uranus.

The low-energy proton intensities are reasonably symmetric about periapsis, despite the apparent offset in the magnetic field (3), but the low-energy electrons (Fig. 2A) exhibit a distinct asymmetry. There appears to be a "shoulder" in the intensity profile of electrons beyond ~ 1400 SCET on 25 August with no similar counterpart in the low-energy protons. The asymmetry is manifested clearly in the electron spectral index, which becomes softer after ~ 1400 SCET; there is no such feature before periapsis. The

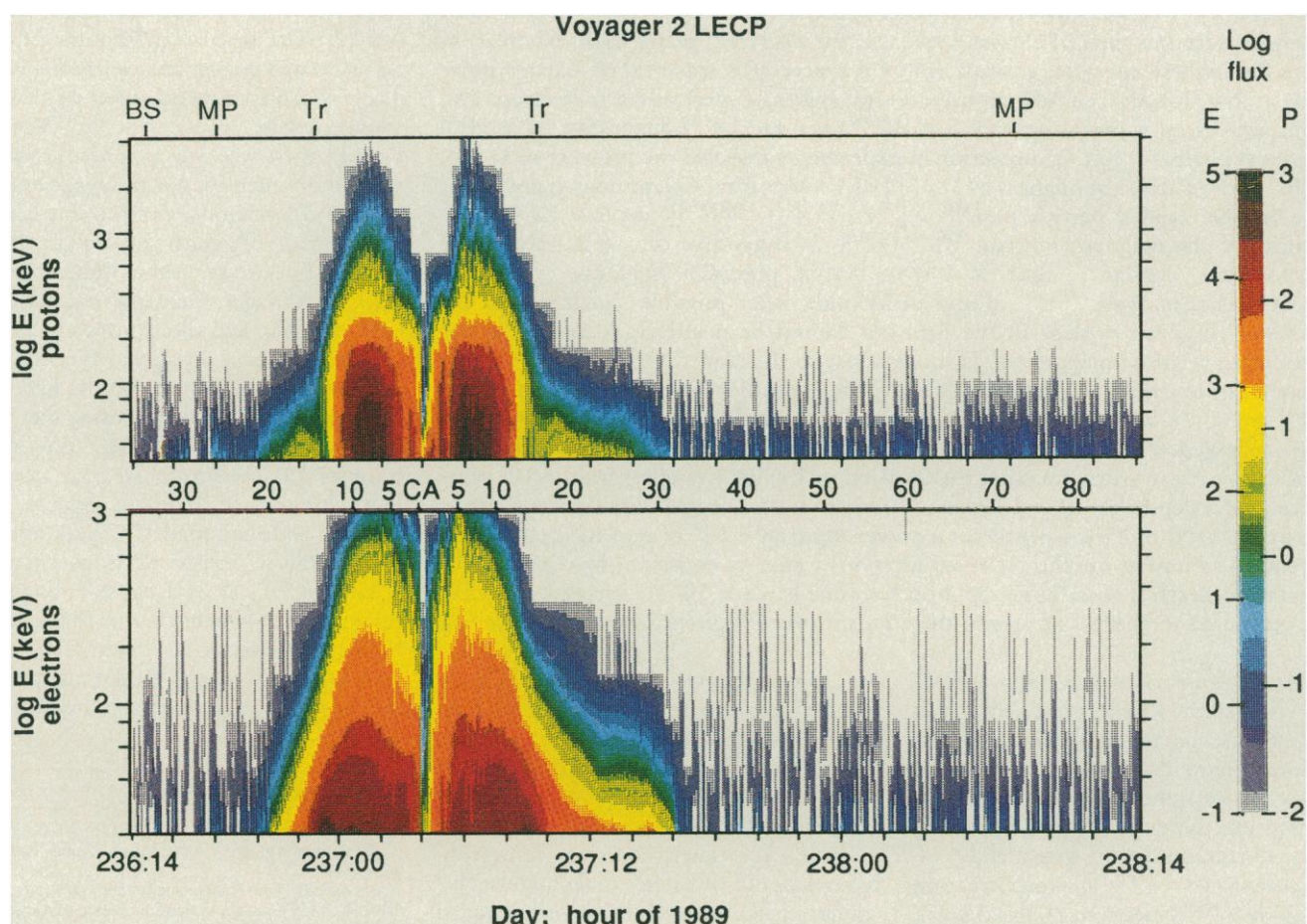


Fig. 1. Spectrogram of energetic ions (top) and electrons (bottom) from 24 August (day 236) 1400 to 26 August (day 238) 1400 SCET. The BS, magnetopause MP, and Triton (Tr) orbit crossing times are shown on top and radial distance in units of planetary radii ($1 R_N = 24,765$ km) are noted

in the middle. The electron fluxes are generally much greater than the proton fluxes at a given energy throughout the encounter (the different color-scaling levels for protons and electrons are shown to the right of the figure).

dropout in the intensity of electrons at ~ 1600 SCET is quite abrupt and, together with the spectral index before this time, suggests that Voyager 2 crossed out of a magnetosphere boundary layer or the "last closed-field line" as it entered what appeared to be the tail lobe of Neptune's magnetosphere.

Two other decreases in the intensity of ~ 250 keV electrons are notable, at ~ 0310 and 0508 SCET, with less pronounced counterparts in the low- and high-energy protons. These are tentatively identified as being caused by 1989N1, as these decreases are in the general vicinity of the appropriate L (that is, the equatorial crossing distance of the magnetic dipole field line measured in planetary radii) value (~ 4.75), per predictions of the offset tilted dipole model (3). There is a softening in the electron spectrum at both times, similar to that seen at the crossing of Triton's orbit.

High-latitude passage. A principal feature of Voyager 2's encounter with Neptune was the close flyby distance of ~ 4900 km over the planet's north pole (4). This flyby geometry allowed us to examine the high-latitude extent of any radiation belts and to measure precipitating electrons and protons that would produce possible auroral emissions. The intensity profile in Fig. 3 is from the same four LECP channels as in Fig. 2, but at higher time resolution for the interval surrounding closest approach. Again, periods of possible electron contamination in the 28-keV proton channel have been deleted. As previously mentioned, the LECP detector heads were rotated to two different "parking" positions during the interval around closest approach (sector 7, generally pointed from $\sim 50^\circ$ to $\sim 90^\circ$ to the radius vector before closest approach, and sector 1, always viewing a direction 90° to sector 7, was pointing generally downward throughout). Because of these changes in viewing direction, discontinuities due to directional effects are seen in the intensities and are easily discernible in the plot, since they occur in periods centered at 6 and 12 min.

In attempting to understand the intensity profiles shown in Fig. 3, it is useful to draw analogies with the known variations of particle intensities measured from a low-altitude polar-orbiting spacecraft in the Earth's magnetosphere (5). In the lowest (ion) curve in Fig. 3 there are two sharp intensity decreases at ~ 0325 SCET and ~ 0510 SCET; these are reminiscent of the latitudinal extent (the high-latitude boundaries) of trapped protons in the Earth's radiation belt. The abruptness of the decrease inbound at ~ 0325 SCET and the gradual increase after ~ 0510 SCET are likely due to the fact that the magnetic field magnitude is

Fig. 2. Counting rates of selected LECP-detector channels averaged over 96 s, together with the electron spectral index γ (A) derived from the expression $dI/dE = KE^{-\gamma}$ over the indicated energy interval. (B) Some of the low-energy ion data [second curve in (B)] have been deleted because of possible electron contamination. The two intensity levels evident on each curve after ~ 0100 SCET on day 237 are due to different orientations of the LECP detector and constitute a rough measure of particle anisotropy. Crossing times of the BS, MP, Triton (Tr), and closest approach (CA) distances are shown on top, together with a radial distance scale in R_N .

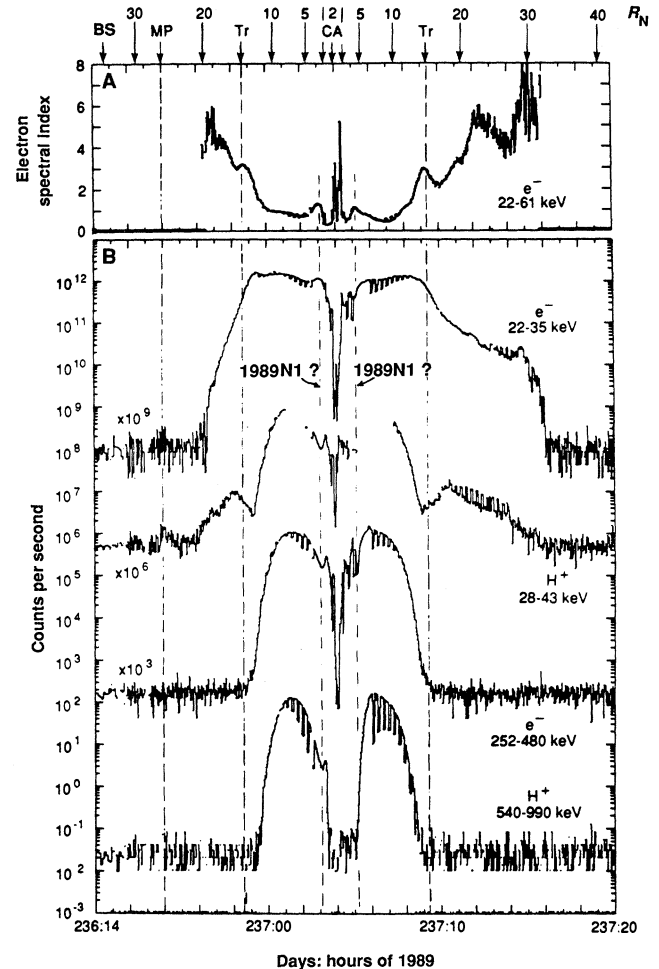
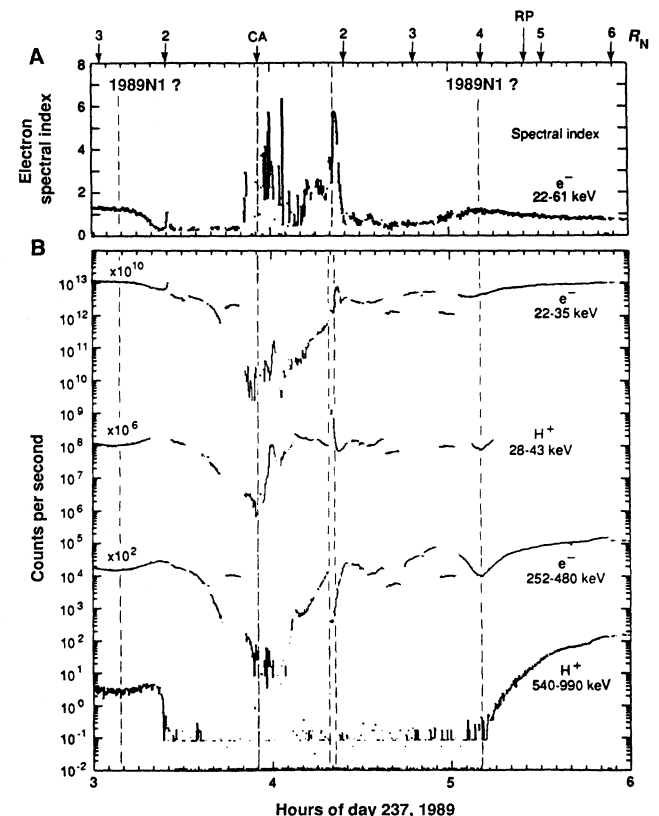


Fig. 3. Counting rates of selected channels, as in Fig. 2, but at 12-s time resolution. A radial distance scale in R_N and the ring plane (RP) crossing outbound are labeled at the top of the figure. An intensity signature most likely caused by satellite 1989N1 is marked. Vertical lines at closest approach and at the time of the ion-electron spike at ~ 0420 SCET are drawn to guide the eye.



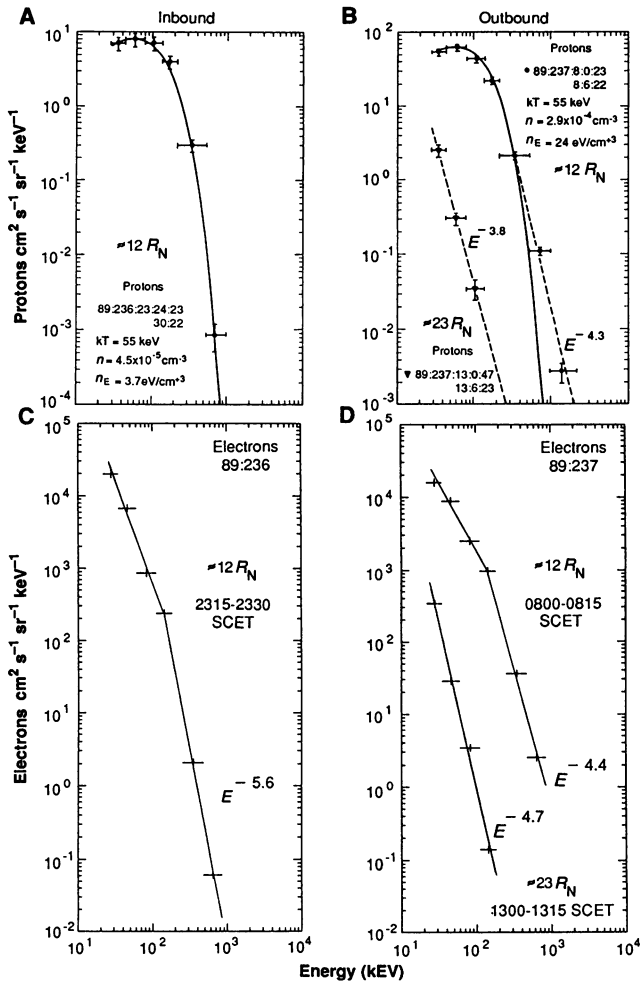


Fig. 4. Differential energy spectra of ions [(A) and (B)] and electrons [(C) and (D)] at selected times inbound [(A) and (C)] and outbound [(B) and (D)]. Note the difference in functional form inside and outside Triton's orbit [(B) and (D), respectively].

probably quite different between inbound and outbound portions of the trajectory (3) because of the dipole offset and associated atmospheric effects. In this sense, the high-energy proton profile thus defines a pass through the high-latitude ($\geq 60^\circ$) region of Neptune's magnetosphere. The second intensity curve from the bottom (high-energy electrons) (Fig. 3B) exhibits a behavior similar to that expected from outer-zone radiation-belt electrons at Earth: a gradual increase occurs near the location of the high-energy proton dropouts. The sharp discontinuities observed between sectors 7 and 1 (for example, 0345 SCET and 0455 SCET) suggest that at these times there may be a change in the electron pitch angle distributions, to ones sharply peaked at $\sim 90^\circ$.

There is considerable variability in the low-energy electron and proton intensities (Fig. 3B, first and second curves from the top, respectively) in this interval. In particular, there are as many as four distinct spikes in the low-energy electron profile between ~ 0350 to ~ 0405 SCET that are not associated with changes in viewing directions. The proton intensity profile exhibits similar variability, but there is only one clearly defined intensity spike (centered at 0400 SCET) that occurs slightly earlier than the corresponding electron spike. It is of particular importance to note that in the case of the electron-intensity spike starting at ~ 0400 SCET, a sector change occurred fortuitously at ~ 0403 SCET and the intensity dropped to near background levels. This shows that the intensity of particles moving downward

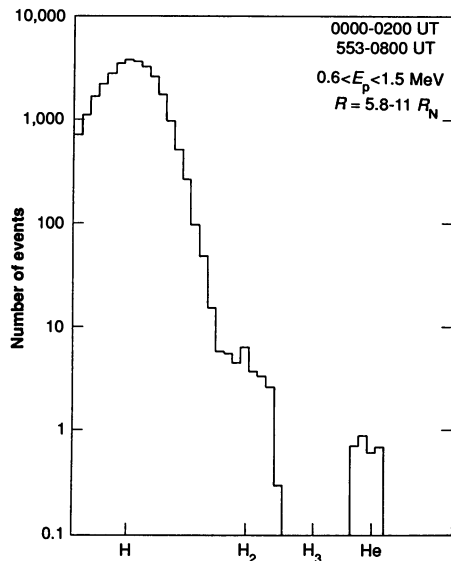


Fig. 5. Logarithmic histogram of pulse-height analyzed events in the low-energy particle telescope (LEPT) system. The shoulder to the right of the proton distribution indicates the presence of H_2 ions in the magnetosphere of Neptune. Because counts are summed along theoretical particle tracks in the matrix of pulse-height events, it is possible to allocate partial counts in a particular bin at low rates, as is evident in the He^+ peak. UT, universal time (same as SCET).

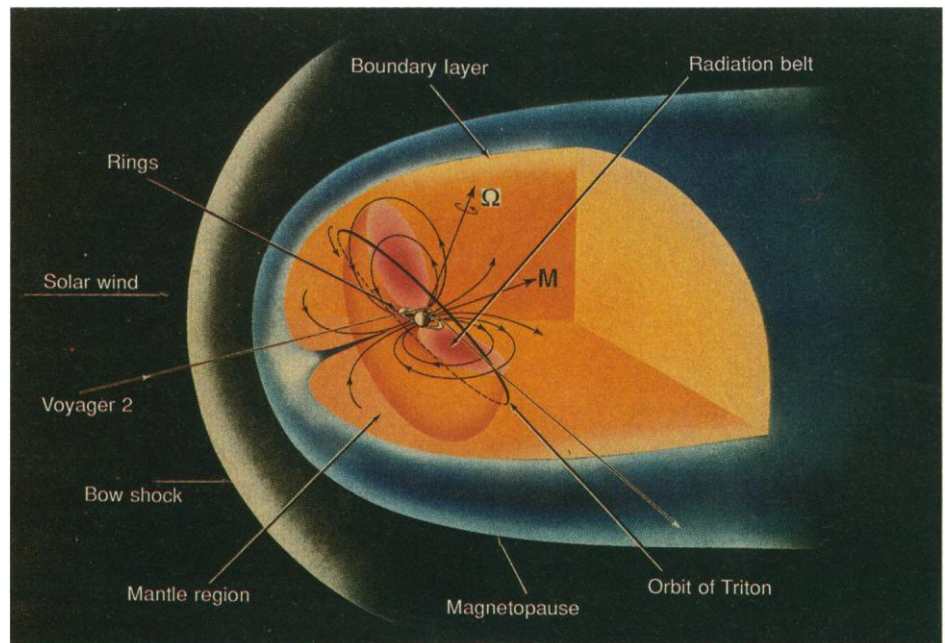


Fig. 6. Conceptual model of Neptune's magnetosphere as it might appear at the time of Voyager's entry through the cusp region. Principal features include the mantle region of semi-trapped particles, the radiation belt delineated by the orbit of Triton, and a boundary layer on the nightside.

from high altitudes was at least a factor of ten higher than the corresponding intensity ~ 0.4 s later at 90° to that direction. We cannot yet report on the pitch angles of these particles, pending detailed magnetic-field information.

The spike in the proton intensity at ~ 0420 SCET is followed by an apparently similar spike of low-energy electrons ~ 2 min later. This proton pulse coincides with a clear deficit in the intensity of ~ 250 -keV electrons. This event was temporal in nature even though there was a change in detector-viewing direction at this time; both sectors 1 and 7 were pointing downward and at roughly the same angle to the radius vector. The special nature of the electron spikes is particularly evident in the spectral variations shown Fig. 3A. The electron spectrum became quite soft for the period ~ 0350 to ~ 0425 SCET, not unlike spectral variations that are observed in the auroral zones of Earth.

The overall impression from the high-latitude trajectory of Voyager 2 is that of passage of the spacecraft from a region of magnetically trapped radiation into a magnetic polar-cap region. Such a passage at Earth also occurs with considerable electron and ion precipitation activity and a softness of the electron spectrum on either side of the higher energy proton-trapping boundary. It is also possible that the spacecraft traversed a region that may map into the location of Triton's flux tube in the outer magnetosphere of Neptune. In this connection, the general softness of the spectrum outside the hard trapping boundary is similar to that observed at Saturn (6), and the possibility exists that Triton may well have a similar role in the magnetosphere of Neptune to that of Titan in the magnetosphere of Saturn.

In Fig. 3 we again saw the decreases potentially associated with 1989N1. A full time-resolution (0.4 s) plot around closest approach reveals a plethora of intensity features potentially associated with the moons and rings discovered by Voyager (4). The absence of an accurate magnetic-field model close to the planet, however, precludes reliable identification of these signatures with specific objects.

Energy spectra and composition. The energy spectra of the electrons varied systematically throughout the encounter, as is evident from the spectral indices shown in Figs. 2 and 3. Inspection of proton spectra shows that this species also had significant spectral variations throughout the magnetosphere. Some characteristic differential energy spectra for ions (protons) and electrons are shown in Fig. 4. The inbound-proton spectrum inside the radial distance of Triton

(Fig. 4A) is well represented by a thermal (Maxwellian) distribution over the entire energy range measured by the LECP instrument. This distribution is characterized by an exceptionally hot temperature $kT \approx 55$ keV (k , Boltzman constant; T , temperature in degrees kelvin) and very low number density (typically 3 to 30×10^{-4} cm^{-3}) and energy density of 3 to 30 eV/ cm^3 . Spectra from the outbound trajectory are shown in Fig. 4B. The spectrum at ~ 0800 SCET is inside the orbit of Triton and shows a nonthermal, high-energy power-law tail with a power-law exponent $\gamma \approx 4$ to 5 . However, the proton spectrum outside the Triton radial distance (~ 1300 SCET), is a simple power law with $\gamma \approx 4$. The corresponding number and energy densities of protons in the range of LECP are only about 2 to 8×10^{-6} cm^{-3} and 0.1 to 0.9 eV/ cm^3 , respectively.

The electron spectra in Fig. 4, C and D are different from those of the protons. A differential spectrum acquired inbound, inside the orbit of Triton is shown in Fig. 4C. The spectrum bends over slightly at the lower energies, and falls off at higher energies with $\gamma \approx 5.6$. The electron spectrum is similar at a corresponding time outbound (that is, inside the orbit of Triton): it bends over at the lower energies and has a high-energy power-law tail with $\gamma \approx 4.4$. In contrast, the electron spectrum outside the orbit of Triton (Fig. 4D) is a simple power law with $\gamma \approx 4.7$. The electron spectrum is not that different from the proton spectrum during the same time interval.

In addition to ion spectral measurements at low energies, the LECP instrument is designed to perform detailed composition measurements at higher ion energies (≥ 0.5 MeV per nucleon.) The results of the composition measurements in Neptune's magnetosphere, averaged over the indicated time intervals when Voyager 2 was within $11 R_N$ of the planet, are as shown in Fig. 5. A proton peak is clearly evident, showing protons to be the dominant ions present. In addition, there is a shoulder in the distribution at the expected location of H_2 molecular ions. Further, there is a small peak containing three counts at the location of He^4 . Only a single heavier ion ($Z > 5$) was observed above 0.5 MeV per nucleon within $11 R_N$, so we cannot determine heavy ion composition. Both H_2 and H_3 molecular ions were measured by LECP in both the magnetospheres of Jupiter and Saturn (6), and H_2 ions were observed in the magnetosphere of Uranus (7). Such molecular ions are expected to come from the ionospheres of those planets and thus serve as tracers for the identification of magnetospheric plasma sources of planets (8). The measured abun-

dances over equal energy per nucleon intervals (0.57 to 1.00 MeV per nucleon) are $\text{H}:\text{H}_2:\text{He}^4$ in the proportion $1300:1:0.1$, with uncertainties of 26% and 62% in the H_2 and He^4 values, respectively. Such a high proton to helium ratio rules out the solar wind (where $\text{H}:\text{He}^4$ ratio is typically ~ 20) as an important source of the plasma in Neptune's magnetosphere.

Discussion. Conclusive interpretation of the energetic particle and hot-plasma measurements made in Neptune's magnetosphere requires a description of the magnetic field; such a model is not available at the present time at distances less than $\sim 4 R_N$ (3). Based upon our preliminary analyses, however, it is possible to draw some general inferences and deduce several important conclusions.

We first wish to compare, in general terms, the magnetosphere of Neptune with the magnetospheres of Uranus and Saturn. Owing to the $\sim 47^\circ$ dipole tilt angle of Neptune's magnetic moment with respect to its rotation axis (3), the magnetosphere of Neptune was nearly in a pole-on configuration when Voyager crossed the magnetopause inbound (Fig. 6). Such was the configuration anticipated for Uranus before the Voyager encounter (9), but not actually achieved because of the large (60°) Uranian dipole tilt and the peculiar orientation of the Uranian rotation axis, pointing nearly toward the sun. At present, the nearly pole-on configuration at Neptune occurs once per Neptune rotation, so it was fortuitous that Voyager at Neptune made the first measurements in the cusp region of an outer-planet magnetopause. The large Neptunian dipole tilt also implies that the satellites of Neptune, like those of Uranus, trace complicated trajectories in the magnetic field, each satellite encountering a large range of L -shells and magnetic latitudes. As a result, a strong geometric dilution occurs that reduces the effects of satellite sources of plasma relative to ionospheric and atmospheric sources (10). A more detailed study of satellite interactions is deferred pending additional information on the magnetic field. It is significant that the ion-abundance ratios reported here for Neptune are very similar to those reported for Uranus (7), indicating the dominance of planet-associated sources in both cases. At Neptune, however, there is some indication of a heavy ion component in the cold plasma (11), contrasting with the case at Uranus, where no heavy ions were detected.

We have made a preliminary calculation of plasma stresses in the Neptune magnetosphere from LECP data. The maximum pressure on the Voyager trajectory was found near day 237 hour 0100 and is nearly

equal, within a factor of two, to that measured in the analogous region of the Uranus magnetosphere (1986 day 24 hour 13, near $L = 12$). The ratio β of plasma to magnetic pressure at Neptune was evaluated as $\beta \approx 0.19$ at the inbound magnetic equator crossing, which occurred on 25 August at ~ 0115 SCET near $L = 10$, close to the region of maximum plasma stress. The cited time for the Uranus encounter also coincided with a magnetic equator crossing, and the Uranian $\beta \approx 0.13$ at that time (12). At Neptune, the $\beta \approx 0.19$ at the inbound magnetic equator crossing is close to the maximum value of β on the Voyager trajectory. This implies that at Neptune, like at Uranus, the local plasma stresses do not significantly distort the magnetic field from a vacuum configuration. This contrasts with the situation at Jupiter and Saturn, where $\beta > 1$ is typically true in the plasma sheet and a strong magnetodisk distortion of the magnetic field results.

Spectral and anisotropy signatures in the magnetosphere of Neptune are similar to those of Saturn, with the moon Triton having a role similar to that of Titan. For example, the energy spectra in the vicinity of Triton's orbit are quite soft, with the high-energy proton and electron intensity gradients occurring just inside the orbits of Triton, both inbound and outbound. Typically, energetic particles are lost because of wave-particle interactions at cold-plasma density gradients, for example, the case of Jupiter's Io plasma torus, Saturn's plasma torus, and the Earth's outer plasmasphere (13, 14). A heavy ion plasma, presumably from Triton, has been detected (11), but Triton's interaction with the magnetosphere is not fully understood as yet (15).

The observation of auroral-like emissions from Triton's atmosphere (N^+ and N_2) (16) suggests that energetic electrons and ions in the vicinity of Triton are incident upon the satellite's atmosphere and excite the emissions. A preliminary estimate of the energy input from LECP-measured energetic electrons is ~ 0.4 erg cm^{-2} s^{-1} , resulting in a total power level of $\sim 10^9$ W. An interaction of the trapped particles with a hypothetical Triton torus could drive the auroral processes, which apparently occur over Neptune's high-latitude region. In fact, the particle observations described in Fig. 3 are consistent with a power input of $\sim 5 \times 10^{-4}$ ergs cm^{-2} s^{-1} . If one assumes that the Neptune auroral zone has a radius of $\sim 10^\circ$, then the total power input into the atmosphere is of the order $\sim 3 \times 10^7$ W, surprisingly small when compared to the magnetospheric energy input into the upper atmospheres of Jupiter, Saturn, and Uranus. Of course, it is quite possible that a substantial flux of precipitating electrons with energies below the

LECP threshold (that is, < 22 keV) may provide more power. This, however, has not been reported as yet (11). Another possibility is that the spacecraft did not traverse a fully developed auroral form, hence the low observed intensities. We note, however, that the estimated radio luminosity from Neptune (17) is substantially lower than similar radio emissions from the other outer planets encountered by Voyager. The possibility of Neptune auroral precipitation events reaching 50-keV energies was anticipated before the encounter (18), but it is premature to state whether inverted V events have been observed at Neptune. Also, chorus and hiss emissions associated with aurora were seen during closest approach (19). The concept of a Neptunian magnetosphere strongly coupled to Triton is summarized in Fig. 6, which presents the principal regions of such a magnetosphere as deduced from the LECP measurements.

There are several additional interesting observations made by the LECP instrument. The instrument did not detect either upstream ion events or energetic charge-exchange neutrals outside the Neptunian magnetosphere. This contrasts with the situation at Earth, Jupiter, and Saturn, where both upstream ion bursts and energetic charge-exchange neutrals were detected at great distances [hundreds of planetary radii for the Voyager spacecraft at Jupiter and Saturn, outside the BS (2, 20, 21)]. At Uranus, on the other hand, upstream ion events but not charge-exchange neutrals were detected (22). Since upstream ion events are observed only when the interplanetary magnetic field (IMF) connects the spacecraft to the BS, and since before the Neptune encounter the IMF lay near the nominal spiral direction (3) ($\sim 90^\circ$ to the planet-sun line), it is likely that this is the reason for nondetection of upstream events. Furthermore, the escape of magnetospheric particles, the dominant process responsible for upstream events, occurs primarily at low magnetic latitudes; Voyager apparently entered and left the Neptune magnetosphere at very high latitudes. This was not the case at Jupiter, Saturn, or Uranus.

Energetic neutral atom fluxes produced by charge exchanges within planetary magnetospheres can be observed by the LECP instrument as a systematic excess count rate in the sector facing the planet when compared with side-looking sectors at background levels if there is an absence of solar events and upstream ion events. The IMF orientation before the Neptune encounter was ideal for detection of energetic neutrals, but none were detected. The upper limit to the flux of neutrals, was $< 2.8 \times 10^{-3}$ cm^{-2} s^{-1} keV^{-1} near 35 keV at $\sim 40 R_N$, about

one-third the flux limit obtained at Uranus (22). Given the observed low-energy (~ 35 keV) proton distributions within $R \leq 6 R_N$ at Neptune, an upper limit can be obtained for the volume averaged atomic H density (\bar{n}) in this region: $\bar{n} \approx 20$ cm^{-3} at Neptune. No extended atomic H corona on Neptune was detected by the ultraviolet spectroscopy (UVS) instrument (16) in contrast to the situation at Uranus (23), where atomic H was observable in Ly α emissions out to $\sim 5 R_U$.

In Neptune's magnetosphere, charged-particle bombardment of satellites and rings can produce a variety of chemical and physical alterations of the solid surfaces (24, 25). Depending on the surface composition, both erosion (sputtering), and discolorations can occur over time. The depth of modification of a surface will depend on the energies of the incident charged particles. Preferential removal of volatiles can result in the production of nonvolatile crusts. Material removed from moons and rings can become plasma sources in the magnetosphere, such as in the cases of Jupiter and Saturn.

We have made a preliminary estimate of the rate of darkening for a surface containing methane ice at the location of 1989N1 around Neptune in the present radiation environment as measured by LECP. Such a surface condition might occur under several circumstances, including exposure of fresh ice after a meteoroid impact. We have found that the darkening rates, to depths of order ~ 10 μm , are similar to those found in the Uranian system at the locations of the moons Umbriel and Ariel (26). That is, darkening to an albedo of perhaps 10% (removal of about 50% of the hydrogen from the methane) will occur to a depth of ~ 1 μm within 10^4 to 10^5 years. Similar darkening to 10 μm will occur within $\sim 3 \times 10^5$ to $\sim 2 \times 10^6$ years. Thus, the dark materials of the ring particles and inner satellites, which continue at present to be radiation-processed by the Neptune magnetosphere, could have been introduced within the last million years just as easily as in the earliest days of the solar system.

In addition to the production of aurora on Triton, the incident radiation on the satellite's atmosphere can produce new chemical species (27) and, for those electrons energetic enough to reach the surface, can produce modifications similar to those previously described of any organic materials located on the surface. At the present epoch, for a pressure at the surface of Triton of ~ 10 μbar , only electrons with ≥ 500 keV of energy at the top of the atmosphere will reach the surface. The primary particles and secondary electrons produced just above the surface will modify the surface materials.

For a 0.5 μ bar (5 μ bar) atmosphere, electrons at initial energy ≥ 70 keV (≥ 300 keV) will penetrate to the satellite's surface. Precise estimates of the modifications of Triton's atmosphere and surface, including seasonal variations in the rates, will be reported later.

REFERENCES AND NOTES

1. S. M. Krimigis *et al.*, *Space Sci. Rev.* **21**, 329 (1977).
2. S. M. Krimigis, in *Comparative Study of Magnetospheric Systems* (Centre National d'Etudes Spatiales, Paris, 1986), p. 99.
3. N. F. Ness *et al.*, *Science*, **246**, 1473 (1989).
4. E. C. Stone and E. Miner, *ibid.*, p. 1417.
5. L. R. Lyons *et al.*, *J. Geophys. Res.* **93**, 12932 (1988).
6. S. M. Krimigis *et al.*, *Science* **212**, 225 (1981); S. M. Krimigis *et al.*, *ibid.* **215**, 571 (1982).
7. S. M. Krimigis *et al.*, *ibid.* **233**, 97 (1986).
8. D. C. Hamilton *et al.*, *Geophys. Res. Lett.* **7**, 813

- (1980).
9. G. L. Siscoe, *Icarus* **24**, 311 (1975).
10. A. F. Cheng, *J. Geophys. Res.* **92**, 15315 (1987).
11. J. W. Belcher *et al.*, *Science* **246**, 1478 (1989).
12. B. H. Mauk *et al.*, *J. Geophys. Res.* **92**, 15283 (1987).
13. M. F. Thomsen *et al.*, *ibid.* **82**, 5541 (1977).
14. A. F. Cheng *et al.*, *ibid.* **90**, 526 (1985).
15. F. M. Neubauer, *Adv. Space Res.*, in press.
16. A. L. Broadfoot *et al.*, *Science* **246**, 1459 (1989).
17. J. W. Warwick *et al.*, *ibid.*, p. 1498.
18. A. F. Cheng, *Geophys. Res. Lett.* **16**, 953 (1989).
19. D. A. Gurnett *et al.*, *Science* **246**, 1494 (1989).
20. R. D. Zwickl *et al.*, *J. Geophys. Res.* **88**, 125 (1981).
21. E. Kirsch *et al.*, *Geophys. Res. Lett.* **8**, 169 (1981); E. Kirsch *et al.*, *Nature* **292**, 718 (1981); A. F. Cheng and R. Johnson, in *Origin and Evolution of Planetary and Satellite Atmospheres*, S. Atreya, J. B. Pollack, M. Matthews, Eds. (Univ. of Arizona Press, Tucson, 1989), p. 682.
22. S. M. Krimigis *et al.*, *Planet Space Sci.* **36**, 311 (1988).
23. A. L. Broadfoot *et al.*, *Science* **233**, 74 (1986).
24. L. J. Lanzerotti, *Nucl. Instrum. Methods* **B32**, 412 (1988).
25. A. F. Cheng *et al.*, in *Satellites*, J. A. Burns and M.

- Mathews, Eds. (Univ. of Arizona Press, Tucson, 1986), p. 403.
26. L. J. Lanzerotti *et al.*, *J. Geophys. Res.* **92**, 14949 (1987).
27. M. L. Delitsky and W. R. Thompson, *Icarus* **70**, 354 (1987); W. R. Thompson, *Geophys. Res. Lett.* **16**, 969 (1989); W. R. Thompson *et al.*, *ibid.*, in press.
28. We thank the members of the Voyager project and personnel at the Jet Propulsion Laboratory and the Planetary Programs Office, NASA Headquarters, for help and cooperation in carrying out this experiment. We thank R. B. Decker, C. Paranicas, M. Kane, B. J. Hook, J. G. Gunther, and J. Green for their enthusiasm and long hours in support of the LECP Voyager project. The help of E. Miner, P. deVries, and O. Divers (among many others) was essential to the success of our investigation. We are also grateful to J. Belcher, D. Gurnett, N. Ness, and E. Stone for discussions concerning the interpretation of the data. The work at The Johns Hopkins University Applied Physics Laboratory was supported by NASA under Task I of Contract N00039-89-C-5301, N00039-89-C-0001, and by subcontracts at the Universities of Kansas and Maryland.

31 October 1989; accepted 15 November 1989

Energetic Charged Particles in the Magnetosphere of Neptune

E. C. STONE, A. C. CUMMINGS, M. D. LOOPER, R. S. SELESNICK, N. LAL, F. B. McDONALD, J. H. TRAINOR, D. L. CHENETTE

The Voyager 2 cosmic ray system (CRS) measured significant fluxes of energetic (≥ 1 megaelectron volt (MeV)) trapped electrons and protons in the magnetosphere of Neptune. The intensities are maximum near a magnetic L shell of 7, decreasing closer to the planet because of absorption by satellites and rings. In the region of the inner satellites of Neptune, the radiation belts have a complicated structure, which provides some constraints on the magnetic field geometry of the inner magnetosphere. Electron phase-space densities have a positive radial gradient, indicating that they diffuse inward from a source in the outer magnetosphere. Electron spectra from 1 to 5 MeV are generally well represented by power laws with indices near 6, which harden in the region of peak flux to power law indices of 4 to 5. Protons have significantly lower fluxes than electrons throughout the magnetosphere, with large anisotropies due to radial intensity gradients. The radiation belts resemble those of Uranus to the extent allowed by the different locations of the satellites, which limit the flux at each planet.

THE COSMIC RAY SYSTEM (CRS) measured significant fluxes of energetic electrons and protons stably trapped within the magnetosphere of Neptune during the close approach of Voyager 2 on 25 August 1989. The instrument consists of two high-energy telescopes (HETs), four low-energy telescopes (LETs), and an electron telescope (TET), each containing several solid-state detectors designed for the study of interplanetary cosmic rays (1). To allow for measurements over a large range of

possible trapped particle intensities in the previously unknown environment of Neptune's magnetosphere, the instrument was cycled every 192 s between two configurations, and various anticoincidence requirements were disabled to prevent excessive deadtime effects. The instrument operated normally throughout the encounter, and none of the detectors was saturated by high particle fluxes.

The Voyager 2 trajectory past Neptune took the spacecraft over the north pole of the planet within 0.2 planetary radius ($R_N = 24,765$ km) of the cloud tops, by far the closest passage of any planetary encounter during the mission. Experience from the other giant planets led to the expectation of rapidly increasing fluxes of trapped radiation as the planet was approached. In addition,

recent ground-based observations of radio emissions from Neptune suggested an intense radiation belt (2). Since Triton, at $14.3 R_N$, was the closest satellite of Neptune known before the Voyager encounter, such an intense radiation belt seemed possible in the absence of satellite sweeping. In fact, the situation at Neptune is quite different from these expectations before the encounter, with the inner radiation belt being limited to relatively low intensity by satellite sweeping.

Electrons. The counting rate profiles in Fig. 1a, shown versus spacecraft event time (SCET), represent electron fluxes at energies greater than approximately 1, 2.5, and 5 MeV (3). The distance of Voyager 2 from Neptune is indicated at the top of the figure in units of R_N . The flux above 1 MeV began to rise above the cosmic ray background level just inside the orbit of Triton and increased sharply for a period of about an hour. At $\sim 8 R_N$ it leveled off and began to fall to the relatively low values near the planet. The peak flux was observed at $5.5 R_N$ on the outbound leg of the trajectory. Clearly there is considerable spatial structure in the trapped electron flux, which apparently is controlled by the newly discovered satellites and rings within $5 R_N$ from Neptune. The largest satellite, 1989N1, has an orbit (at $4.75 R_N$) and size similar to those of Miranda, the innermost moon of Uranus, which plays an important role in limiting the trapped radiation intensity at that planet.

Because trapped electrons are guided by the magnetic field, it is usual to organize the data by using the magnetic shell parameter, L . Figure 1b shows the spacecraft L versus time in the offset tilted dipole (OTD) model of the planetary magnetic field (4, 5), which incorporates a 46.8° tilt of the magnetic

E. C. Stone, A. C. Cummings, M. D. Looper, R. S. Selesnick, California Institute of Technology, Pasadena, CA 91125.

N. Lal, F. B. McDonald, J. H. Trainor, NASA Goddard Space Flight Center, Greenbelt, MD 20771.

D. L. Chenette, Lockheed Palo Alto Research Laboratory, Palo Alto, CA 94304.